Posttetanic potentiation critically depends on an enhanced Ca^{2+} sensitivity of vesicle fusion mediated by presynaptic PKC

Natalya Korogod*†‡, Xuelin Lou*§, and Ralf Schneggenburger*†¶

*AG Synaptic Dynamics and Modulation, Department of Membrane Biophysics, Max–Planck–Institute for Biophysical Chemistry, D-37077 Göttingen, Germany; and †Laboratory of Synaptic Mechanisms, Brain-Mind Institute, École Polytechnique Fédérale de Lausanne, 1015 Lausanne, Switzerland

Edited by Richard W. Tsien, Stanford University School of Medicine, Stanford, CA, and approved August 10, 2007 (received for review May 16, 2007)

Activity-dependent enhancement of transmitter release is a common form of presynaptic plasticity, but the underlying signaling mechanisms have remained largely unknown, perhaps because of the inaccessibility of most CNS nerve terminals. Here we investigated the signaling steps that underlie posttetanic potentiation (PTP), a form of presynaptic plasticity found at many CNS synapses. Direct whole-cell recordings from the large calyx of Held nerve terminals with the perforated patch-clamp technique showed that PTP was not mediated by changes in the presynaptic action potential waveform. Ca^{2+} imaging revealed a slight increase of the presynaptic Ca^{2+} transient during PTP (≈15%), which, however, was too small to explain a large part of PTP. The presynaptic PKC pathway was critically involved in PTP because (*i*) PTP was occluded by activation of PKC with phorbol esters, and (*ii*) PTP was largely (by approximately two-thirds) blocked by the PKC inhibitors, Ro31-8220 or bisindolylmaleimide. Activation of PKC during PTP most likely acts directly on the presynaptic release machinery, because in presynaptic Ca^{2+} uncaging experiments, activation of PKC by phorbol ester greatly increased the Ca^{2+} sensitivity of vesicle fusion in a Ro31-8220-sensitive manner (≈300% with small Ca^{2+} uncaging stimuli), but only slightly increased presynaptic voltage-gated Ca^{2+} currents (≈15%). We conclude that a PKC-dependent increase in the Ca^{2+} sensitivity of vesicle fusion is a key step in the enhancement of transmitter release during PTP.

readily releasable pool | second messenger | short-term plasticity | synapse | synaptic plasticity

Synaptic transmission at chemical synapses is the main means of information transfer among neurons in the brain. Transmission is not static but can be modulated by activity on various time scales, giving rise to short-term plasticity (1) and longer-lasting forms of synaptic plasticity (2). Posttetanic potentiation (PTP) is an enhancement of transmitter release on a minute time scale (3–5), which is most likely induced by the buildup of spatially averaged, residual Ca^{2+} in the nerve terminal during high-frequency firing periods (6–9). There is general agreement that the residual Ca^{2+} signal, with an amplitude of a few hundred nanomolar (1), is too small to directly increase the release probability by summation with the local Ca^{2+} signal that triggers vesicle fusion because the Ca^{2+} signal relevant for vesicle fusion has a much higher amplitude (≈10–20 μM $[Ca^{2+}]_i$) (10, 11). Thus, one explanation for the action of residual Ca^{2+} in short-term enhancement assumes that residual Ca^{2+} binds to a high-affinity site associated with the release apparatus, but distinct from the Ca^{2+} sensor for vesicle fusion (1, 12). Alternatively, it has been suggested more recently that residual Ca^{2+} could activate second-messenger pathways in the nerve terminal, which in turn potentiate transmitter release (13, 14), and, indeed, PKC has been implicated in PTP (13, 15).

It is not known with certainty how transmitter release is ultimately increased during presynaptic forms of plasticity. In principle, both the number of readily releasable vesicles as well as their release probability (*P*) could be increased. An increase in *P* could be caused by an enhanced Ca^{2+} influx [e.g., broadening of the presynaptic action potential (AP)] (16–18). In the absence of enhanced Ca^{2+} influx, *P* could still be increased by reduced intracellular Ca^{2+} buffering (19, 20), by an increased Ca^{2+} channel–vesicle coupling, or by an increase in the Ca^{2+} sensitivity of vesicle fusion (21). A distinction among these mechanisms at CNS synapses would be greatly facilitated by direct electrophysiological recordings from nerve terminals during synaptic enhancement. The calyx of Held is a giant glutamatergic synaptic terminal in the auditory brainstem, at which pre- and postsynaptic recordings can be performed (22, 23) and which expresses, like many other synapses, robust PTP (14, 18). Here we use a combination of presynaptic perforated whole-cell recordings, presynaptic Ca^{2+} uncaging, and pharmacological tools to investigate which presynaptic signaling steps are altered during PTP and how the presynaptic PKC pathway is involved in PTP.

Results

PTP Is Not Caused by AP Broadening. A broadening of the presynaptic AP can increase the presynaptic Ca^{2+} influx (16, 17) and thereby enhance release probability. To investigate whether AP broadening underlies PTP (18), we made paired pre- and postsynaptic whole-cell recordings by using Nystatin-perforated patch recording of the presynaptic nerve terminal (Fig. 1). This process was necessary because, under conventional presynaptic whole-cell recordings, PTP is not observed (14). In Fig. 1*A*, the protocol for inducing PTP, and example traces of presynaptic APs and excitatory postsynaptic currents (EPSCs) are shown. The baseline synaptic strength was first assessed by low-frequency stimulation (every 10 sec; Fig. 1*A*, black traces). Thereafter, a high-frequency (100-Hz) train of 4-sec duration was given to induce PTP, followed by low-frequency stimulation to test for the development of synaptic strength. The first EPSC after the 100-Hz train was strongly depressed, but over the next 20–30 sec, EPSCs recovered and then transiently increased

Author contributions: N.K. and X.L. contributed equally to this work; N.K., X.L., and R.S. designed research; N.K. and X.L. performed research; N.K. and X.L. analyzed data; and R.S. wrote the paper.

The authors declare no conflict of interest.

This article is a PNAS Direct Submission.

Abbreviations: AP, action potential; BIS, bisindolylmaleimide I; EPSC, excitatory postsynaptic current; mEPSC, miniature EPSC; PDBu, phorbol 12,13-dibutyrat; PTP, posttetanic potentiation.

‡Present address: Université de Lausanne, CH-1015 Lausanne, Switzerland.

§Present address: Department of Cell Biology and Howard Hughes Medical Institute, Yale University School of Medicine, New Haven, CT 06520-8002.

¶To whom correspondence should be addressed. E-mail: ralf.schneggenburger@epfl.ch.

This article contains supporting information online at www.pnas.org/cgi/content/full/0704603104/DC1.

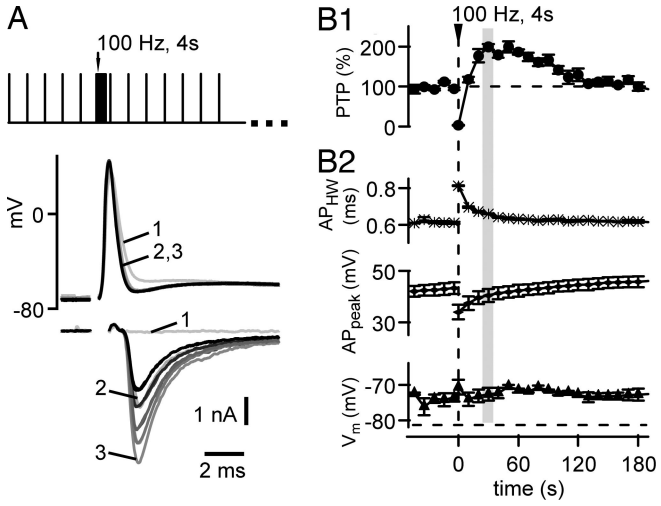

Fig. 1. Broadening of the presynaptic AP waveform does not contribute to PTP. (*A*) Presynaptic APs (*Upper*) and corresponding EPSCs (*Lower*) in response to fiber stimulation, recorded under presynaptic perforated patch-clamp conditions. (*Inset*) Stimulation protocol used to induce and test for PTP. Black and gray traces were obtained before and after induction of PTP, respectively. The first three EPSCs and APs after PTP induction are indicated. (*B1*) Time course of PTP (average of $n = 4$ repetitions) in the same cell as shown in *A*. (*B2*) Time course of AP half width (*Top*), the absolute AP amplitude (*Middle*), and resting membrane potential (*Bottom*) measured before each AP. At the peak of PTP (≈30 sec after the train; see gray bar), the changes in AP half-width and AP amplitude have decayed back to baseline.

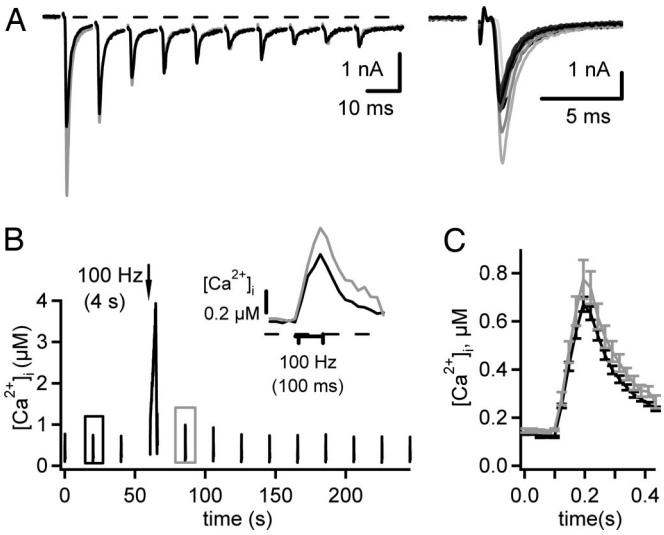

Fig. 2. The presynaptic Ca^{2+} influx is slightly increased during PTP. EPSCs and presynaptic Ca^{2+} transients in response to brief trains of fiber stimuli (10 times, 100 Hz) were recorded before and after the induction of PTP. (*A*) Superimposed EPSCs in response to brief trains before (black traces) and after the induction of PTP (gray traces). (*Inset*) Each first EPSC. (*B*) Presynaptic Ca^{2+} transients measured from the corresponding calyx of Held that was preloaded with ≈80–100 μM fura-4F. (*Inset*) Expanded example traces recorded before (black) and after (gray) the induction of PTP (see boxes in *B*). (*C*) Average Ca^{2+} transients from $n = 7$ inductions in three cells showing a slight amplitude increase.

≈2-fold over their baseline amplitude (Fig. 1*A* and *1B*), characteristic of PTP at this (14, 18) and other synapses (1, 4). The amplitude of PTP was 192 ± 9% in this cell ($n = 4$ inductions; Fig. 1*B*) and 167 ± 11% across cells under these recording conditions ($n = 4$). Thus, under perforated whole-cell recordings of the presynaptic nerve terminal, PTP is preserved, which allowed us to investigate whether the presynaptic AP waveform is changed during PTP.

In the example in Fig. 1*A*, the first AP after the 100-Hz induction train was slightly broadened. Later APs, however, were virtually unchanged compared with the APs before the 100-Hz induction train. Analyzing the half width of the AP and its absolute amplitude (Fig. 1*B2 Top* and *Middle*, respectively) showed some change of these parameters immediately after the 100-Hz train, but at the time when PTP was maximal (≈30 sec after the induction train), the width and amplitude of the presynaptic AP had largely relaxed back to their control values. On average, the AP half widths were 0.53 ± 0.05 and 0.55 ± 0.06 msec before and 30 sec after the PTP induction trains, respectively, and, thus, were not changed significantly ($P = 0.77$; $n = 4$ cell pairs). In addition, we did not observe a change in the resting membrane potential measured before each AP (Fig. 1*B2 Bottom*; −69.7 ± 1.9 and −69.3 ± 1.4 mV before and at the peak of PTP; $n = 4$ cells; $P = 0.84$), ruling out the possibility that a subthreshold depolarization of the nerve terminal (24) might cause PTP. A short-lasting (≈1 sec) posttetanic hyperpolarization of the nerve terminal (25) was not picked up in our experiments and should not be relevant for PTP, which is maximal 20–30 sec after the high-frequency train. Thus, although AP broadening occurs after PTP-induction trains, it decays before PTP is maximal, making a role for AP broadening during PTP unlikely.

A Small Increase in Presynaptic Ca^{2+} Influx During PTP. Although AP broadening did not significantly contribute to PTP, it is possible that other mechanisms (e.g., a modulation of presynaptic voltage-gated Ca^{2+} channels) could cause an increase in the presynaptic Ca^{2+} influx. To test whether an increase in the presynaptic Ca^{2+} current contributes to PTP, we initially made paired recordings with perforated presynaptic whole-cell recordings under voltage clamp. Under these conditions, however, we did not observe PTP [see supporting information (SI) Fig. 6]. To assess whether PTP is accompanied by changes in presynaptic Ca^{2+} influx, we imaged $[Ca^{2+}]_i$ in calyces of Held briefly preloaded with a Ca^{2+} indicator (fura-4F) and measured PTP in response to afferent fiber stimulation in postsynaptic recordings, an experimental condition under which PTP can be stably observed (14, 26). We applied short 100-Hz trains with 10 stimuli to measure the synaptic strength (by using the first EPSC in each train) (Fig. 2*A Right*) and image the presynaptic $[Ca^{2+}]_i$ signal associated with each brief 100-Hz train (Fig. 2*B*). After three repetitions of such test stimuli applied every 20 sec, a 4-sec, 100-Hz train was given to induce PTP, and the test stimuli were applied again every 20 sec. The $[Ca^{2+}]_i$ transients associated with a test stimulus before and 20 sec after the induction train are superimposed in Fig. 2*B Inset* (black and gray traces, respectively). The amplitude of the $[Ca^{2+}]_i$ signal was larger after the induction of PTP (774 ± 81 nM) than under control conditions (671 ± 30 nM; $n = 7$ inductions in three cells) (Fig. 2*C*, gray and black average traces, respectively). On average, the presynaptic $[Ca^{2+}]_i$ transient was increased to 115 ± 4% of its control value, which is in agreement with a recent report (26). If the ≈15% increase of the Ca^{2+} transient was caused by a similar increase of the local Ca^{2+} signal relevant for vesicle fusion, then a transmitter release potentiation of ≈150% of control could result, assuming a third-power relation between transmitter release and local Ca^{2+}. However, this is probably an upper limit estimate because not all of the 15% increase in the global Ca^{2+} transient might be relevant for transmitter release (see *Discussion*).

Involvement of Presynaptic PKC Signaling in PTP. The findings that (*i*) PTP is accompanied only by a small increase in Ca^{2+} influx (≈15%) (Fig. 2) (26), and (*ii*) an increase in the size of the readily

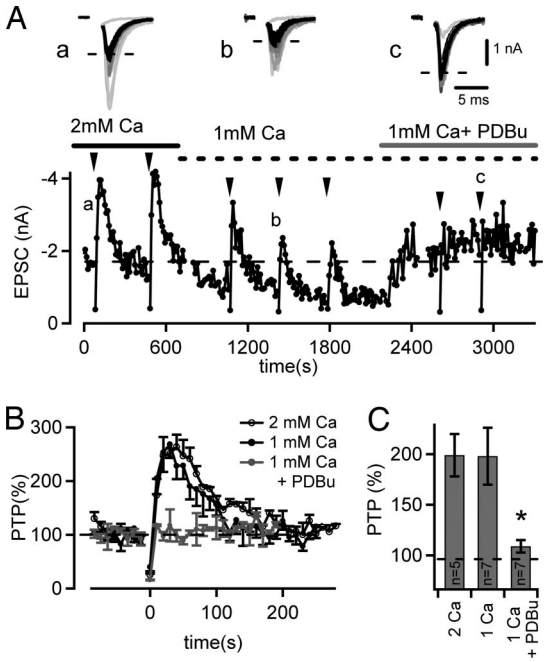

Fig. 3. PTP- and phorbol ester-induced potentiation of transmitter release share a common pathway. (*A*) Time plot of EPSC amplitudes for a typical experiment. PTP was induced repetitively by 4-sec, 100-Hz trains (see arrowheads) in the presence of 2 mM extracellular $[Ca^{2+}]$, at 1 mM $[Ca^{2+}]$, and finally after application of 1 μM PDBu in the presence of 1 mM $[Ca^{2+}]$. Note that PDBu increased the baseline EPSC amplitude and led to the disappearance of PTP. (*Inset*) Example EPSCs recorded before (black) and after (gray) each PTP induction for the three different recording conditions. (*B*) Time course of PTP for the cell shown in *A* for the three different recording conditions as indicated (average traces for $n = 2$ inductions each). (*C*) Average PTP summarized for the conditions tested here (2 mM $[Ca^{2+}]$, $n = 5$ cells; 1 mM $[Ca^{2+}]$, $n = 7$ cells; 1 mM $[Ca^{2+}]$ in the presence of 1 μM PDBu, $n = 7$ cells) (*, $P < 0.01$, Student's *t* test).

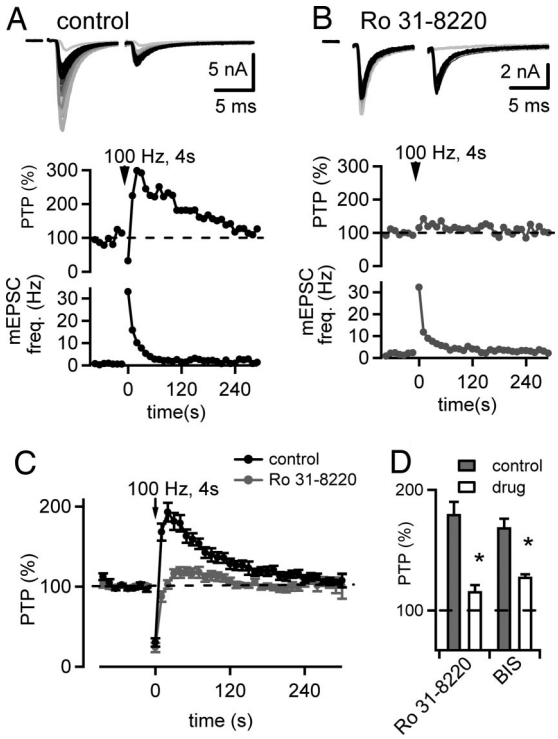

Fig. 4. PTP is suppressed by the PKC inhibitors Ro31-8220 and BIS. (*A*) PTP in a control cell. Example EPSC traces before (black) and after (*Top*, gray) PTP induction, the time course of PTP (*Middle*), and the time course of mEPSC frequency (*Bottom*). (*B*) Similar to *A*, but with EPSCs recorded from another cell preincubated for >30 min with 3 μM Ro31-8220. (*C*) Average time course of relative EPSC amplitudes (shown as the percentage of baseline) summarized for control cells (black circles, $n = 7$ cells) and for the Ro31-8220 group (gray circles, $n = 15$ cells). (*D*) Amplitude of PTP for control cells (gray bars) and for cells in the presence of Ro31-8220 (open bars) (control, $n = 7$; drug, $n = 15$). Acute application of 10 μM BIS (control, $n = 13$; drug, $n = 13$) also reduced PTP. Asterisks indicate statistical significance of the drug group versus the corresponding control group ($P < 0.01$).

releasable vesicle pool during PTP induced by 100-Hz trains of a few seconds is negligible (14) indicate that an increase in the Ca^{2+} sensitivity of vesicle fusion might critically contribute to PTP. Interestingly, PKC has been implicated in PTP (13, 15), and activation of the presynaptic PKC pathway by phorbol esters has been shown to enhance the Ca^{2+} sensitivity of vesicle fusion (21, 27). We therefore investigated a possible involvement of PKC in PTP in an occlusion experiment, asking, first, whether PTP can be induced after potentiating transmitter release by phorbol esters (Fig. 3), which activate PKC (28) as well as the active-zone protein munc-13 (29). In these experiments, PTP was induced in regular intervals by 4-sec, 100-Hz stimulus trains (Fig. 3*A*, arrowheads). After having established PTP under control conditions in the presence of 2 mM $[Ca^{2+}]$, we lowered the extracellular $[Ca^{2+}]$ to 1 mM to compensate for the expected increase in transmitter release probability induced by phorbol esters. Under lowered extracellular $[Ca^{2+}]$, the amplitude of PTP was not significantly different from the one under control conditions ($199 \pm 21\%$, $n = 5$; $198 \pm 28\%$, $n = 7$ for 2 and 1 mM $[Ca^{2+}]$, respectively; $P > 0.5$) (see Fig. 3*C*). In the presence of 1 mM $[Ca^{2+}]$, we then applied 1 μM phorbol 12,13-dibutyrate (PDBu), which potentiated the baseline EPSC amplitudes and led to a nearly complete disappearance of PTP (Fig. 3 *A* and *B*). In the presence of PDBu, PTP was only $109 \pm 6\%$ ($n = 7$ cells) of the control synaptic strength, significantly smaller than PTP measured at 1 mM $[Ca^{2+}]$ ($198 \pm 28\%$; $P < 0.01$) (Fig. 3*C*). This finding suggests that the activation of PKC by phorbol ester occludes the dynamic increase in transmitter release that underlies PTP.

We next asked whether PTP is sensitive to blockers of PKC (13, 15). Slices were incubated in control solution or with 3 μM Ro31-8220, and the amount of PTP was compared between the slices (Fig. 4 *A* and *B*). Two example recordings of EPSCs before and after the 100-Hz induction trains are shown in Fig. 4 *A* and *B Top*. The corresponding relative PTP and miniature EPSC (mEPSC) frequency are shown in Fig. 4 *A* and *B*, *Middle* and *Bottom*, respectively. On average, PTP was $193 \pm 12\%$ ($n = 7$ cells) under control conditions (Fig. 4*C*, black average symbols), but only $116 \pm 5\%$ ($n = 15$ cells) in slices preincubated with 3 μM Ro31-8220 (Fig. 4*C*, gray symbols), significantly smaller than under control conditions ($P < 0.001$) (Fig. 4*D*). However, the increase in mEPSC frequency immediately after the 100-Hz train was similar in both groups (19 ± 6 and 15 ± 6 Hz for control and with Ro31-8220, respectively; $P > 0.5$) (Fig. 4 *A* and *B Bottom*). Preincubation with 3 μM Ro31-8220 did not significantly change the baseline EPSC amplitudes (control, 5.1 ± 1.9 nA, $n = 7$ cells; Ro31-8220, 6.2 ± 0.6 nA, $n = 15$ cells; $P > 0.1$), suggesting that there is no constitutive PKC activity important for maintaining the baseline synaptic strength. Acute application 10 μM bisindolylmaleimide I (BIS), another PKC blocker, also significantly suppressed PTP (control, $168 \pm 7\%$; BIS, $119 \pm 6\%$, $n = 13$ cells; $P = 0.008$) (see Fig. 4*D*).

Activation of PKC Leads to an Increase in the Ca^{2+} Sensitivity of Vesicle Fusion. The suppression of PTP by Ro31-8220 and BIS shows that a large part (approximately two thirds) of PTP depends on the activation of the presynaptic PKC pathway (Fig.

4*C*). However, it is not known whether activation of PKC during PTP primarily acts on the vesicle fusion machinery (e.g., by increasing the Ca^{2+} sensitivity of vesicle fusion) (21, 27) or whether PKC primarily modulates voltage-gated Ca^{2+} channels, an effect that could explain the slightly increased Ca^{2+} influx after the induction of PTP (Fig. 2) (26). To investigate these possibilities, it would be ideal to measure presynaptic Ca^{2+} currents and the Ca^{2+} sensitivity of vesicle fusion (using presynaptic Ca^{2+} uncaging) before and after the induction of PTP. However, this process requires presynaptic whole-cell recording, a condition under which PTP is not observed (14). We circumvented this experimental difficulty by activating PKC/munc-13 with the phorbol ester PDBu, and asked whether the resulting increase in the Ca^{2+} sensitivity of vesicle fusion as measured by Ca^{2+} uncaging (21) is sensitive to the PKC blocker, Ro31-8220. In addition, this experiment allowed us to investigate the degree of Ca^{2+} current modulation by PKC activation.

Simultaneous pre- and postsynaptic whole-cell recordings were made, and transmitter release was evoked by weak presynaptic Ca^{2+} uncaging stimuli (Fig. 5 *A* and *D*), as well as by brief (≈1-msec) presynaptic depolarizations from −80 to 0 mV (Fig. 5 *C* and *F*). In a control cell pair in the absence of Ro31-8220 (Fig. 5*A*), the application of 1 μM PDBu strongly increased the EPSC evoked by Ca^{2+} uncaging (≈3.5-fold in the example in Fig. 5*A*), despite a virtually unchanged presynaptic Ca^{2+} signal (Fig. 5*A Top*). At the same time, PDBu strongly increased the depolarization-evoked EPSC (Fig. 5*C Bottom*), with an average potentiation to 681 ± 213% of the control amplitude (n = 4 cells) (Fig. 5*G*, open bar). This potentiation of the EPSC amplitude was accompanied by only a small increase of the presynaptic voltage-gated Ca^{2+} current (Fig. 5*C Top*), with average potentiation to 114 ± 3% of control (Fig. 5*H*, open bar). Thus, phorbol ester strongly potentiated transmitter release irrespective of whether release was evoked by depolarizations or by Ca^{2+} uncaging, but voltage-gated Ca^{2+} currents were only slightly increased. Therefore, the main action of phorbol ester application must be a direct modulation of the presynaptic vesicle fusion machinery (21, 27).

To investigate the contribution of PKC activation to these effects, we repeated similar experiments in slices preincubated with 3 μM Ro31-8220 (Fig. 5 *D–F*). Under these conditions, transmitter release evoked by Ca^{2+} uncaging was still potentiated by PDBu (≈2.2-fold in the example in Fig. 5*D*), but the potentiation was significantly smaller when analyzed over all cells (Fig. 5*I*). Similarly, the potentiation of EPSCs evoked by brief presynaptic depolarizations was only 210 ± 40%, significantly smaller than under control conditions (P = 0.048) (Fig. 5*G*, gray bar).

To analyze the potentiation of the Ca^{2+} uncaging-evoked release in more detail, we deconvolved the EPSCs to obtain transmitter release rates (30). For the cell shown in Fig. 5*A*, this analysis indicated an ≈3.5-fold potentiation of the peak transmitter release rate by PDBu (Fig. 5*A Bottom*). The peak release rates before and after the application of PDBu were plotted as a function of the presynaptic $[Ca^{2+}]_i$ reached after the flashes (Fig. 5*B*). In this plot, the peak release rates obtained after PDBu potentiation were higher than the control release rates at the corresponding $[Ca^{2+}]_i$, and the relative potentiation decreased with $[Ca^{2+}]_i$ stimuli of increasing amplitudes (Fig. 5*B*, black and gray data points). This finding is compatible with our previous finding that phorbol esters enhance the Ca^{2+} sensitivity of vesicle fusion concomitant with a reduction in the steepness of the relationship between transmitter release rates and $[Ca^{2+}]_i$ (21).

In slices preincubated with 3 μM Ro31-8220 (Fig. 5*D*), the data points obtained before and after application of PDBu largely superimposed (Fig. 5*E*), indicating that the potentiation of the Ca^{2+} sensitivity of vesicle fusion was less efficient under Ro31-8220. We next analyzed the relative potentiation in each

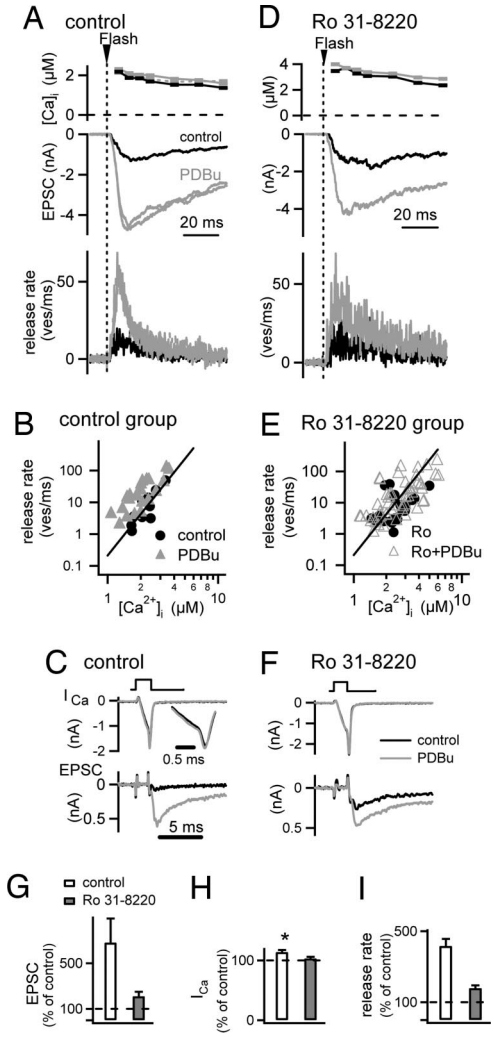

Fig. 5. The phorbol ester-induced increase in the Ca^{2+} sensitivity of vesicle fusion is suppressed by the PKC blocker Ro31-8220. Paired pre- and postsynaptic conventional whole-cell recordings coupled with presynaptic Ca^{2+} uncaging are shown. (*A*) Presynaptic $[Ca^{2+}]_i$ step induced by Ca^{2+} uncaging (*Top*), EPSCs (*Middle*), and transmitter release rates resulting from EPSC deconvolution (*Bottom*) both before and after application of 1 μM PDBu (black and gray traces, respectively). (*B*) Plot of peak transmitter release rates as a function of the $[Ca^{2+}]_i$ increase after flashes before (black symbols) and after (gray symbols; n = 7 cell pairs) application of PDBu. The line indicates a slope of 4.2 in double-logarithmic coordinates. (*C*) Presynaptic Ca^{2+} currents (*Upper*) and EPSCs (*Lower*) before (black traces) and after (gray traces) application of PDBu. (*D–F*) Similar experiment and analysis as in *A*, *B*, and *C*, but in a slice preincubated with 3 μM Ro31-8220. (*G*) Average potentiation of the depolarization-evoked EPSCs by PDBu under control conditions (open bar, n = 4 cells) and in cells preincubated with Ro31-8220 (gray bar; n = 6 cells). (*H*) Average potentiation of presynaptic Ca^{2+} current amplitude under control conditions (open bar; n = 4 cells) and in the presence of Ro31-8220 (gray bar; n = 6 cells). Asterisk indicates statistically significant difference from 100% (P = 0.048). (*I*) Average relative increase of transmitter release rates for presynaptic Ca^{2+} uncaging stimuli in the range of 1–4 μM. Note the significantly smaller ($P < 0.001$) increase in transmitter release rates in the presence of Ro31-8220 (gray bar, n = 7 cells) as compared with control (open bar; n = 4 cells).

cell by calculating the increase of each data point measured in the presence of PDBu relative to the corresponding x value of a line with a slope of 4.2 (see Fig. 5 *B* and *E*, straight line), which was shifted on the x axis to best fit the control data points in each cell (see ref. 19). This analysis showed a relative potentiation of transmitter release rates of 394% ± 36% of control in the absence of Ro31-8220 (n = 22 flashes in n = 4 cells; range, 1–4

μM $[Ca^{2+}]_i$) (Fig. 5*I*, open bar). In the presence of 3 μM Ro31-8220, the relative potentiation was only 179% ± 16% in the same range of $[Ca^{2+}]_i$ ($n = 43$ flashes in $n = 7$ cell pairs) (Fig. 5*I*, open bar), significantly smaller than that measured under control conditions ($P < 0.001$). These experiments show that activating PKC by phorbol esters enhances transmitter release, to a large part, by directly increasing the Ca^{2+} sensitivity of vesicle fusion.

Discussion

We have studied the presynaptic signaling mechanisms and the role of PKC in PTP, a transient increase in transmitter release observed in many synapses after periods of high-frequency activity. Using perforated whole-cell recordings of the large calyx of Held nerve terminals, we found that presynaptic AP broadening occurs after PTP-inducing stimuli, but largely recovers before PTP is maximal (Fig. 1), suggesting that AP broadening does not significantly contribute to PTP induced by brief (≈4-sec) 100-Hz trains. Ca^{2+} imaging experiments revealed a slight (≈15%) increase of the presynaptic Ca^{2+} transient after PTP-inducing stimuli (Fig. 2) (26). An increase in the spatially averaged Ca^{2+} signal can, in principle, be caused by (*i*) some remaining AP broadening, (*ii*) a modulation of voltage-gated Ca^{2+} currents, and (*iii*) a reduced intracellular Ca^{2+} buffering strength, including buffer saturation of the indicator dye (31). Because we do not know which fraction of the ≈15% increase in the Ca^{2+} transient is relevant for transmitter release, it is difficult to estimate its exact contribution to PTP at present.

Several lines of evidence indicate a critical role for presynaptic PKC in PTP. Thus, potentiating transmitter release by the phorbol ester PDBu occluded PTP (Fig. 3), and the PKC inhibitors Ro31-8220 and BIS strongly suppressed PTP (Fig. 4) (13). However, the PKC inhibitors did not decrease the basal synaptic strength, indicating either (*i*) that PKC is not activated under basal conditions, or (*ii*) that a constitutive PKC activity, if it exists, is not necessary for maintaining transmitter release. Therefore, it is most plausible to assume that PTP-inducing stimuli activate presynaptic PKC. Because diacylglycerol and phorbol esters can activate the active-zone protein munc-13 (29, 32), in addition to their classical action on PKCs (33), the occlusion of PTP by phorbol ester could also indicate an involvement of munc-13. Indeed, there is evidence that activation of munc-13 underlies part of the phorbol ester potentiation at the calyx of Held (28) (X.L., N.K., A. Betz, N. Brose, and R.S., unpublished data). However, PTP was blocked by Ro31-8220 and BIS, ATP-site inhibitors of PKC (34), which should not affect munc-13, suggesting that primarily PKC, and not munc-13, is involved in PTP.

It is likely that activated PKC increases the probability of transmitter release primarily by increasing the Ca^{2+} sensitivity of vesicle fusion during PTP. It has been shown previously at the calyx of Held that the main action of phorbol esters is an increase in the Ca^{2+} sensitivity of vesicle fusion (21, 27), with only a small (21) or no apparent effect (27, 28) on presynaptic voltage-gated Ca^{2+} currents. Here we showed that the phorbol ester-induced increase in the Ca^{2+} sensitivity of vesicle fusion is partially mediated by PKC because this effect is sensitive to Ro31-8220 (Fig. 5). Phorbol esters increase the transmitter release probability without an increase in the size of a readily releasable vesicle pool as probed by strong presynaptic depolarizations (21, 27), and PTP induced by 100-Hz trains was also not accompanied by a marked pool size increase (ref. 14, but see ref. 35). Taken together, the main effect of PKC activation is likely a direct effect on the release machinery that acts to increase the apparent Ca^{2+} sensitivity of vesicle fusion (21). In addition, we showed that PKC activation by phorbol ester causes a weak, Ro31-8220-sensitive potentiation of voltage-gated Ca^{2+} currents (Fig. 5 *C* and *H*). However, it is difficult at present to assess the relevance of this small Ca^{2+} channel modulation for transmitter release because it is not known whether P/Q-, N-, or R-type channels, which are present at young calyces of Held (36, 37) and couple with different efficiencies to transmitter release (37), are affected by the modulation.

PKC might be activated during PTP-inducing stimuli either directly by Ca^{2+} binding to their C2 domains (in the case that conventional PKCs are involved) (33) and/or by binding of diacylglycerol to the C1 domains, but the signaling pathways leading to an increase in diacylglycerol by presynaptic activity are unclear at present. Activated PKC likely phosphorylates a target protein in the vesicle fusion machinery, like munc-18 (38, 39), which in turn might lead to an increase in the Ca^{2+} sensitivity of vesicle fusion. Other presynaptic proteins, like SNAP-25 and synaptotagmin-1, also have PKC phosphorylation sites (40–42), but are less likely candidates (43–45). It is possible that PKC becomes activated by each PTP-inducing train and subsequently phosphorylates a presynaptic target protein, and that the decay of PTP represents the dephosphorylation of the target protein. Alternatively, a constitutive PKC phosphorylation of some presynaptic target proteins might be permissive for the induction of PTP. In this case, however, one would have to assume that a constitutive PKC activity should be selectively permissive for the dynamic increase of transmitter release during PTP, but leave the basal synaptic strength unaffected because Ro31-8220 did not affect the basal EPSC amplitudes.

Our data suggest that activation of presynaptic PKC during repetitive firing in nerve terminals enhances the Ca^{2+} sensitivity of vesicle fusion, and thereby causes a short-term enhancement of transmitter release. Thus, the increase in the Ca^{2+} sensitivity of vesicle fusion that underlies the potentiation of transmitter release by phorbol esters (21) can also be targeted by physiological activity in the nerve terminal. A modulation of the Ca^{2+} sensitivity of vesicle fusion, independent from possible changes in the size of the readily releasable pool, thus emerges as an important mechanism that allows intracellular second messengers to enhance the efficiency of transmitter release during presynaptic plasticity.

Materials and Methods

Slice Preparation, Electrophysiology, and Solutions. Native brainstem slices of 200-μm thickness, containing the region of the medial nucleus of the trapezoid body, were made by using 7- to 10-day-old rats. Young rats were used because PTP is more easily induced compared with more mature animals (14). The slices were kept (<5 h) in a chamber at 36°C, which was later allowed to cool to room temperature. The chamber contained a solution (125 mM NaCl/25 mM $NaHCO_3$/2.5 mM KCl/1.25 mM NaH_2PO_4/1 mM $MgCl_2$/2 mM $CaCl_2$/25 mM glucose/0.4 mM ascorbic acid/3 mM myo-inositol/2 mM Na-pyruvate) continuously bubbled with 95% O_2/5% CO_2 (pH 7.4). Recordings were made at room temperature (21–24°C) under visual control with an upright microscope (FS2; Carl Zeiss, Oberkochen, Germany) or Olympus BX51-WI (Hamburg, Germany) equipped with a ×60 objective (Olympus) and gradient contrast illumination (Luigs & Neumann, Ratingen, Germany). Whole-cell patch-clamp recordings were made with a double EPC-10 amplifier (HEKA Elektronik, Lambrecht, Germany). Series resistance (R_s) was 3–10 MΩ for postsynaptic and 8–25 MΩ for conventional presynaptic recordings, respectively, and was compensated by 50–85%. The pipette solution for postsynaptic recordings contained 130 mM Cs-gluconate, 20 mM tetraethylammonium-Cl, 20 mM Hepes, 5 mM EGTA, 5 mM Na_2-phosphocreatine, 4 mM MgATP, and 0.3 mM Na_2GTP. The extracellular solution was the same as the slice-keeping solution. For the experiments shown in Fig. 5, 1 μM tetrodotoxin, 10 mM tetraethylammonium, 50 μM D-2-amino-5-phosphonovalerate, and 100 μM cyclothiazide were added. For some experiments shown in Figs.

4 and 5, the slices were preincubated for at least 30 min with 3 μM Ro31-8220 (Calbiochem, Hofheim, Germany) in a small incubation chamber (≈25-ml volume). For the subsequent recordings after Ro31-8220 preincubation, the drug also was present in all perfusion solutions. BIS (Calbiochem, San Diego, CA) was applied acutely to slices after obtaining one to two PTP inductions under control conditions.

Recording Configurations. The following combinations of recording configurations were used: (*i*) paired presynaptic current-clamp and postsynaptic voltage-clamp recordings, using presynaptic perforated (Nystatin) recordings (Fig. 1). The experiments in SI Fig. 6 were similar but under presynaptic voltage-clamp conditions. (*ii*) Postsynaptic voltage-clamp recordings with simultaneous presynaptic Ca^{2+} imaging of a calyx of Held preloaded with ≈80–100 μM fura-4F (Fig. 2) (14). (*iii*) Postsynaptic voltage-clamp recordings (Figs. 3 and 4). (*iv*) Paired presynaptic voltage-clamp recordings and postsynaptic voltage-clamp recordings with additional presynaptic Ca^{2+} uncaging (Fig. 5). For the experiments shown in Figs. 1–4, the synapses were stimulated by afferent fiber stimulation with a bipolar stimulation electrode placed between the midline of the slice and the medial nucleus of trapezoid body.

Presynaptic Perforated Patch Recordings. Nystatin (0.2 mg/ml) was added to an intracellular solution containing 150 mM K-gluconate, 20 mM KCl, and 25 μM fura-2 (pentapotassium salt; Molecular Probes, Eugene, OR) by using a freshly prepared stock solution of Nystatin (24 mg/ml; in DMSO). Series resistances of 15–26 MΩ were obtained. The fluorescence of fura-2 was used to verify for spontaneous occurrence of the conventional whole-cell mode. When this occurred, the measurements were discontinued, and data were analyzed only for periods during which the calyx fluorescence was indistinguishable from background fluorescence.

Ca^{2+} Imaging and Ca^{2+} Uncaging. The Ca^{2+}-imaging system was based on a monochromator and a CCD camera (TILL Photonics, Gräfelfing, Germany). For presynaptic Ca^{2+} uncaging (Fig. 5), the presynaptic pipette solution contained 130 mM Cs-gluconate, 20 mM tetraethylammonium-Cl, 20 mM Hepes, 5 mM Na_2ATP, 0.3 mM Na_2GTP, 0.1 mM fura-2FF, 1 mM DM-nitrophen, 0.85 mM $CaCl_2$, and 0.5 mM $MgCl_2$. The Ca^{2+} uncaging was done as described previously (46) by using a flash lamp (Rapp Optoelektronik, Hamburg, Germany).

Analysis of Release Rate and mEPSC Detection. Analysis was performed with routines written in IgorPro (Wavemetrics, Lake Oswego, OR). Transmitter release rates (Fig. 5 *A* and *D Bottom*) were calculated by deconvolving the measured and off-line corrected EPSC traces with an idealized mEPSC waveform by using an EPSC deconvolution procedure (30) similarly as described (46). Spontaneous mEPSCs were detected with a template matching routine. Application of Tetrodotoxin does not change the amplitude distribution of spontaneous EPSCs at the calyx of Held (47). Therefore, we assume that spontaneous EPSCs, which had mean amplitudes of 25–40 pA across cells, represent quantal events (mEPSCs). Results are reported as average ± SEM, and statistical significance was assessed with paired or unpaired *t* tests as appropriate.

We thank Erwin Neher and Takeshi Sakaba for helpful discussions and Nils Brose and Martin Müller for comments on the manuscript. This work was supported by Deutsche Forschungsgemeinschaft (Sonderforschungsbereich SFB-406 and Grants Schn451/4-1 and Schn451/4-2) and a Heisenberg fellowship (to R.S.).

1. Zucker RS, Regehr WG (2002) *Annu Rev Physiol* 64:355–405.
2. Malenka RC, Bear MF (2004) *Neuron* 44:5–21.
3. Liley AW, North KAK (1953) *J Neurophysiol* 16:509–527.
4. Magleby KL, Zengel JE (1975) *J Physiol* 245:163–182.
5. McNaughton BL (1982) *J Physiol* 324:249–262.
6. Swandulla D, Hans M, Zipser K, Augustine GJ (1991) *Neuron* 7:915–926.
7. Regehr WG, Delaney KR, Tank DW (1994) *J Neurosci* 14:523–537.
8. Delaney KR, Tank DW (1994) *J Neurosci* 14:5885–5902.
9. Kamiya H, Zucker RS (1994) *Nature* 371:603–606.
10. Bollmann J, Sakmann B, Borst J (2000) *Science* 289:953–957.
11. Schneggenburger R, Neher E (2000) *Nature* 406:889–893.
12. Junge HJ, Rhee J-S, Jahn O, Varoqueaux F, Spiess J, Waxham MN, Rosenmund C, Brose N (2004) *Cell* 118:389–401.
13. Brager DH, Cai X, Thompson SM (2003) *Nat Neurosci* 6:551–552.
14. Korogod N, Lou X, Schneggenburger R (2005) *J Neurosci* 25:5127–5137.
15. Alle H, Jonas P, Geiger JRP (2001) *Proc Natl Acad Sci USA* 98:14708–14713.
16. Jackson M, Konnerth A, Augustine G (1991) *Proc Natl Acad Sci USA* 88:380–384.
17. Geiger JR, Jonas P (2000) *Neuron* 28:927–939.
18. Habets RLP, Borst JGG (2005) *J Physiol* 564:173–187.
19. Felmy F, Neher E, Schneggenburger R (2003) *Neuron* 37:801–811.
20. Blatow M, Caputi A, Burnashev N, Monyer H, Rozov A (2003) *Neuron* 38:79–88.
21. Lou X, Scheuss V, Schneggenburger R (2005) *Nature* 435:497–501.
22. Forsythe ID (1994) *J Physiol* 479:381–387.
23. Borst JGG, Helmchen F, Sakmann B (1995) *J Physiol* 489:825–840.
24. Awatramani GB, Price GD, Trussell LO (2005) *Neuron* 48:109–121.
25. Kim JH, Sizov I, Dobretsov M, von Gersdorff H (2007) *Nat Neurosci* 10:196–205.
26. Habets RLP, Borst JGG (2006) *J Neurophysiol* 96:2868–2876.
27. Wu XS, Wu LG (2001) *J Neurosci* 21:7928–7936.
28. Hori T, Takai Y, Takahashi T (1999) *J Neurosci* 19:7262–7267.
29. Rhee J-S, Betz A, Pyott S, Reim K, Varoqueaux F, Augustin I, Hesse D, Südhof TC, Takahashi M, Rosenmund C, Brose N (2002) *Cell* 108:121–133.
30. Neher E, Sakaba T (2001) *J Neurosci* 21:444–461.
31. Neher E, Augustine GJ (1992) *J Physiol* 450:273–301.
32. Betz A, Ashery U, Rickmann M, Augustin I, Neher E, Südhof TC, Rettig J, Brose N (1998) *Neuron* 21:123–136.
33. Newman AC (1997) *Curr Opin Cell Biol* 9:161–167.
34. Way KJ, Chou E, King GL (2000) *Trends Pharmacol Sci* 21:181–187.
35. Habets RLP, Borst JGG (2007) *J Physiol* 581:467–478.
36. Iwasaki S, Takahashi T (1998) *J Physiol* 509:419–423.
37. Wu LG, Westenbroek RE, Borst JGG, Catterall WA, Sakmann B (1999) *J Neurosci* 19:726–736.
38. Fujita Y, Sasaki T, Fukui K, Kotani H, Kimura T, Hata Y, Südhof TC, Scheller RH, Takai Y (1996) *J Biol Chem* 271:7265–7268.
39. Wierda KDB, Toonen RFG, De Wit H, Brussard AB, Verhage M (2007) *Neuron* 54:275–290.
40. Shimazaki Y, Nishiki T, Omori A, Sekiguchi M, Kamata Y, Kozaki S, Takahashi M (1996) *J Biol Chem* 271:14548–14553.
41. Nagy G, Matti U, Nehring RB, Binz T, Rettig J, Neher E, Sorensen JB (2002) *J Neurosci* 22:9278–9286.
42. Hilfiker S, Pieribone VA, Norstedt C, Greengard P, Czernik AJ (1999) *J Neurochem* 73:921–932.
43. Finley MFA, Scheller RH, Madison DV (2003) *Neuropharmacology* 45:857–862.
44. Pang ZP, Sun JY, Rizo J, Maximov A, Südhof TC (2006) *EMBO J* 25:2039–2050.
45. Nagy G, Kim JH, Pang ZP, Matti U, Rettig J, Südhof TC, Soerensen JB (2006) *J Neurosci* 26:632–643.
46. Wölfel M, Lou X, Schneggenburger R (2007) *J Neurosci* 27:3198–3210.
47. Ishikawa T, Sahara Y, Takahashi T (2002) *Neuron* 34:613–621.